

TurboMap: GPU-Accelerated Local Mapping for Visual SLAM

Parsa Hosseini¹, Kimia Khabiri¹, Shishir Gopinath¹,
Soudabeh Mohammadhashemi¹, Karthik Dantu², Steven Y. Ko¹

Abstract—This paper presents TurboMap, a GPU-accelerated and CPU-optimized local mapping module for visual SLAM systems. We identify key performance bottlenecks in the local mapping process for visual SLAM and address them through targeted GPU and CPU optimizations. Specifically, we offload map point triangulation and fusion to the GPU, accelerate redundant keyframe culling on the CPU, and integrate a GPU-accelerated solver to speed up local bundle adjustment. Our implementation is built on top of ORB-SLAM3 and leverages CUDA for GPU programming. The experimental results show that TurboMap achieves an average speedup of $1.3\times$ in the EuRoC dataset and $1.6\times$ in the TUM-VI dataset in the local mapping module, on both desktop and embedded platforms, while maintaining the accuracy of the original system.

I. INTRODUCTION

Simultaneous Localization and Mapping (SLAM) systems enable robots to estimate their position and build a map of the environment by processing data from various sensors, including cameras, LiDAR, and inertial measurement units (IMUs). Visual SLAM systems, in particular, rely on visual sensors, typically monocular, stereo, or RGB-D cameras, to reconstruct the environment and localize the robot within it.

A typical visual SLAM pipeline consists of three main components: tracking, local mapping, and loop closing [1]. Tracking estimates the camera pose by extracting features from the current frame and matching them to existing map points, local mapping refines and expands the map to improve accuracy of the system, and loop closing detects revisited locations to correct accumulated drift. Well-known examples of this class of SLAM systems include ORB-SLAM [2], [3], [4], OpenVINS [5], and Kimera [6].

In real-time visual SLAM, each component must operate within strict time constraints, as delays in any stage compromise overall system performance, with local mapping being particularly critical. In systems that maintain a global map, such as ORB-SLAM, falling behind or skipping local mapping results in larger, less accurate maps and a higher risk of tracking loss. Systems without a global map (e.g., Kimera, OpenVINS) avoid immediate tracking failures but experience delayed or missed loop closures. However, because these systems still rely on optimized maps for accurate pose estimation, incomplete local mapping ultimately degrades trajectory quality [1].

To avoid keyframe drops or processing delays in local mapping, which can degrade localization accuracy, incom-

ing keyframes generated by the tracking module must be processed promptly. To address this, we present TurboMap, a GPU-accelerated and CPU-optimized local mapping module for visual SLAM systems. Our approach begins by analyzing local mapping’s computational bottlenecks. We then accelerate these bottlenecks either by offloading their logic to the GPU or by optimizing them on the CPU. For GPU-based tasks, we carefully design kernels and memory management strategies to minimize overhead, such as kernel launch costs and data transfers, ensuring that GPU parallelization yields performance gains.

We select ORB-SLAM3 as our representative visual SLAM system and implement TurboMap on top of it to concretely demonstrate the benefits of our approach.

We compare the local mapping performance of TurboMap with the vanilla ORB-SLAM3 using widely used datasets EuRoC [7] and TUM-VI [8]. Our experiments show that TurboMap achieves an average speedup of $1.3\times$ on the EuRoC dataset and $1.6\times$ on the TUM-VI dataset in the local mapping module compared to ORB-SLAM3, across both desktop and embedded platforms, while maintaining similar trajectory accuracy. Although our implementation is based on ORB-SLAM3, we expect the proposed techniques to generalize to other visual SLAM systems that maintain a global map and implement the components we accelerate in TurboMap. Our code is available at <https://github.com/sfu-rsl/TurboMap>.

II. RELATED WORK

In this section, we briefly discuss related work on GPU acceleration for tracking, local mapping, and loop closing modules in the context of ORB-SLAM based systems [2], [3], [4].

Several studies focus on optimizing the tracking module in SLAM systems. Aldegheri et al. [9] analyze the data flow of ORB-SLAM2 and exploit it to introduce additional levels of parallelism and accelerate feature extraction. Kumar et al. [10] implement bounded rectification for FAST and pyramidal culling and aggregation and introduce a middle-end component for tracking. Khabiri et al. [11] use GPU to accelerate key bottlenecks in the ORB-SLAM3 tracking module, including feature extraction, stereo feature matching, and local map tracking, achieving up to $2.8\times$ speed up in the tracking process on both desktop and embedded platforms.

Other works focus on accelerating least squares subproblems in various modules. Gopinath et al. [12] parallelize matrix calculations to accelerate local bundle adjustment in

¹Simon Fraser University. { sph6, kka156, sgopinath, sma406, steveyko}@sfu.ca

²University at Buffalo. kdantu@buffalo.edu

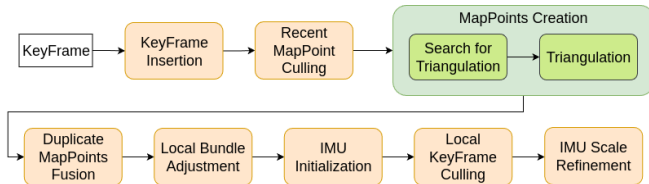


Fig. 1: Local mapping workflow in ORB-SLAM3.

local mapping, while Kumar et al. [13] offload Jacobian computations for pose graph optimization to the GPU. The Ceres Solver [14] introduces optional CUDA-based linear solvers to speed up the optimization steps in bundle adjustment, and MegBA [15] provides a fully GPU-native, distributed BA framework capable of handling large-scale optimizations.

In contrast to previous work, we focus on offloading local mapping tasks aside from bundle adjustment to the GPU. Specifically, we move the logic of map point creation and fusion to the GPU and accelerate redundant keyframe culling on CPU. To support these parallelized GPU algorithms, we also design a dedicated keyframe storage system that efficiently manages the data required by these operations.

III. BACKGROUND

The local mapping module in a visual SLAM system is responsible for processing keyframes as well as building, maintaining, and optimizing the map. The computations performed in this component are critical for ensuring both the efficiency and accuracy of the system. Figure 1 illustrates the different stages of local mapping, using ORB-SLAM3 as an example visual SLAM system. In the rest of the section, we explain each component.

A. Map-point Creation

Map point creation is responsible for estimating the 3D coordinates of 2D keypoints and integrating the resulting 3D points into the map. The system begins by triangulating each keypoint in the current keyframe with the corresponding keypoints in neighboring keyframes to determine their 3D positions. After triangulation, a set of geometric and photometric constraints is evaluated, and new map points are inserted into the map only if these constraints are satisfied. The constraints include sufficient parallax between views, positive depth (i.e. points must lie in front of the camera), low re-projection error, and consistency in scale.

B. Map-point Fusion

Map point fusion aims to eliminate duplicate map points to maintain a cleaner and more accurate representation of the environment. The process begins by retrieving the neighboring keyframes of the current keyframe, including some second-order neighbors. For each map point in the current keyframe, the system searches for the map point most similar to the map point in each retrieved keyframe. If a pair of map points is determined to be sufficiently similar based on geometric and descriptor-based criteria, they are merged, with one of them being discarded. This fusion process helps produce a sparser and more consistent map.

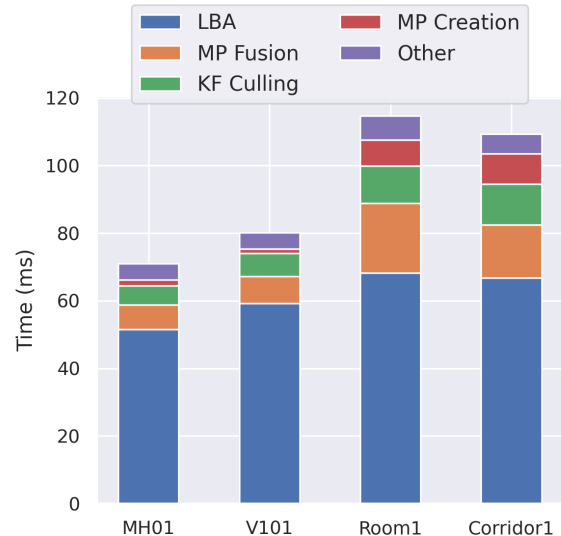


Fig. 2: Average time spent in different sections of local mapping in ORB-SLAM3.

C. Local Bundle Adjustment

Local bundle adjustment (LBA) refines the poses of local keyframes and the positions of the 3D map points observed by them. This process is typically formulated as a nonlinear least-squares problem that minimizes reprojection residuals (and inertial residuals in visual-inertial systems). The optimization is solved iteratively, often using Gauss-Newton or Levenberg-Marquardt methods. To improve efficiency, the large number of point variables is handled via the Schur complement, which eliminates them from the system of equations so that only the smaller set of pose variables is solved directly. The resulting updates to poses and map points reduce local drift and improve trajectory consistency.

D. Local Keyframe Culling

Keyframe culling identifies and removes redundant local keyframes to maintain a compact and efficient map. SLAM systems typically handle this process differently. For example, in ORB-SLAM3, a keyframe is considered redundant if at least 90% of the map points it observes are also seen in three or more other keyframes at the same or finer scale. Removing such non-informative keyframes reduces memory usage and computational overhead, leading to a more efficient system. This process also benefits local bundle adjustment, whose computational complexity increases with the number of keyframes involved.

IV. DESIGN

To reduce the latency of the local mapping process, we focus on optimizing its most time-consuming components. As shown in Figure 2, approximately 95% of the computation time is spent on Map Point Creation, Map Point Fusion, LBA, and Keyframe Culling.

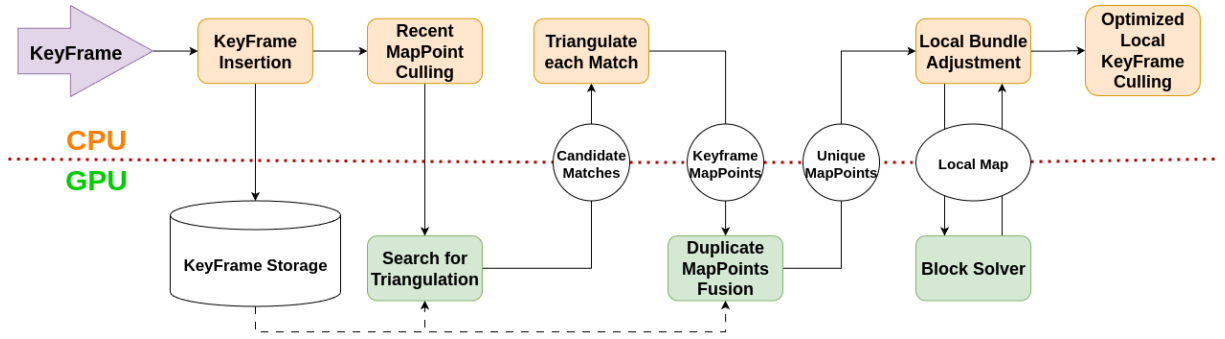


Fig. 3: Data flow of the local mapping process in TurboMap. CPU-side components are shown at the top, and GPU-side components at the bottom. Arrows indicate data transfers between modules. Keyframe storage resides on the GPU.

Figure 3 illustrates the local mapping architecture in TurboMap, showing the division of responsibilities between the CPU and the GPU. We offload a component to the GPU if it meets three key criteria: It has a high computational overhead, exhibits a high degree of parallelism, and requires only a small amount of input data. If any of these conditions are not satisfied, GPU acceleration may offer limited benefits or even introduce additional overhead due to data transfer and synchronization costs. To further enhance performance, we allocate GPU memory during system initialization and release it upon shutdown, minimizing runtime allocation costs. We discuss the different components used in TurboMap in the following sections.

A. System Overview

To explain how TurboMap operates and to highlight its differences and advantages over the original ORB-SLAM3, we present the local mapping flow depicted in Figure 3 using ORB-SLAM3 as the baseline for comparison. The local mapping stage in both systems is triggered when tracking hands a newly created keyframe to it. In ORB-SLAM3 all keyframes are maintained in CPU memory. In contrast, as shown in Figure 3, TurboMap immediately copies each new keyframe to a dedicated GPU storage, enabling subsequent components to access required data without repeated transfers.

The first operation in the pipeline is to remove recently created map points that are redundant or classified as outliers. This check is inexpensive and remains on the CPU with its logic unchanged. The next stage is Map Point Creation, which involves searching for corresponding map points in neighboring keyframes and then performing triangulation. In ORB-SLAM3, both steps are executed sequentially on the CPU, with the search phase dominating the computational cost of this component. In TurboMap we separate these two sub-tasks and offload the correspondence search to the GPU while retaining triangulation on the CPU. Triangulation has negligible per-match cost and would incur unnecessary data movement if performed on the GPU, so keeping triangulation on the CPU provides the best trade-off between computation and transfer overhead. On the other hand, the correspondence search stage is computationally heavy and highly parallelizable, so TurboMap offloads it to the GPU.

After creating new map points, the system performs duplicate map point detection and fusion. Fusion compares candidate descriptors across first-order and selected second-order neighbors to find duplicates, which involves many independent descriptor comparisons. Because fusion is computationally intensive and highly parallelizable, TurboMap offloads it to the GPU, where parallel execution significantly reduces latency compared to the CPU implementation in ORB-SLAM3. The pipeline then performs Local Bundle Adjustment to refine the poses of local keyframes and the positions of associated map points. As one of the primary bottlenecks in local mapping, reducing its latency is essential to achieve faster overall performance. Instead of re-implementing this complex optimizer, TurboMap integrates an existing GPU-accelerated LBA solver [12] and uses it as a drop-in module for ORB-SLAM3’s optimizer. Finally, redundant keyframes are removed by Keyframe Culling. In TurboMap, this stage is redesigned on the CPU rather than ported to the GPU, since it requires frequent access to map point data that are continuously updated during local mapping. Transferring these data to the GPU at each iteration would introduce significant overhead, so TurboMap instead optimizes the CPU implementation to reduce latency.

In the following subsections, we provide a detailed description of each component in TurboMap and the rationale behind its GPU or CPU optimization.

B. Keyframe Storage

Search for Triangulation and Map Point Fusion, the two components which TurboMap offloads to the GPU, frequently need access to map point data from many neighboring keyframes. A naive approach would transfer all required keyframes to the GPU each time a new keyframe is processed. However, this is highly inefficient: Each keyframe is roughly 1 MB, and with tens of neighbors, repeated transfers would introduce substantial overhead. To solve this issue, TurboMap implements a persistent keyframe storage on the GPU. Each keyframe is transferred to the keyframe storage on GPU once when it enters local mapping and remains there until it is removed from the map or the system shuts down, avoiding repeated data transfers and ensuring efficient GPU execution. The keyframe data stored in this storage mainly

include keypoints and their descriptors for each keyframe.

C. Search for Triangulation

As shown in Figure 3, the first component we offload to the GPU is Search for Triangulation. This stage is computationally intensive and highly parallelizable, making it well suited for GPU acceleration with minimal data transfer overhead. During the Search for Triangulation stage, the system attempts to identify the most similar feature in neighboring keyframes for each feature in the current keyframe. This is done by computing the descriptor distance between each pair of features. Additionally, each potential match is validated against epipolar constraints to ensure geometric consistency. Given the high number of features per keyframe and the large number of descriptor comparisons required, this process is computationally expensive. However, since finding the best match for each feature is independent of other features and keyframes, the task is highly parallelizable. To take advantage of this situation, we offload this task to the GPU and task each GPU thread to independently perform descriptor comparisons and verify epipolar constraints. This parallel execution significantly reduces latency, as the workload is distributed across many threads. In terms of the required data, the keyframes represent the largest potential overhead. However, since we use keyframe data that is already stored on the GPU, no additional data transfer is incurred.

D. Map-point Fusion

Duplicate Map Point Fusion is the second component which TurboMap offloads to the GPU as shown in Figure 3. The primary goal of this function is to determine whether there exists a map point in the map that (1) has descriptors very similar to those of a map point associated with the current keyframe and (2) is spatially close to that map point. This process is computationally intensive, highly parallelizable, and benefits from the fact that most of the required data, particularly keyframe-related information, already reside in GPU memory.

The Fuse and Search for Triangulation components share similar logic, as both compute the feature similarities. However, as described in Section III, the Fuse component searches for duplicate map points across first-order and selected second-order neighboring keyframes, whereas Search for Triangulation is limited to first-order neighbors. As a result, the fuse operation is more computationally intensive, which is also evident in Figure 2. This makes Fuse even a better candidate for parallelization. In the GPU implementation, each thread is responsible for identifying the most similar map point to a given point in the current keyframe within a specific neighboring keyframe. Regarding data transfer, the primary data required by this component includes the neighboring keyframes and the map points associated with the current keyframe. The former is already stored on the GPU, incurring no transfer cost, while the latter amounts to approximately 100 KB, which is an insignificant size that has minimal impact on the performance of the GPU program.

E. Local Bundle Adjustment

The final component that TurboMap accelerates by using GPU computation is Local Bundle Adjustment, as illustrated in Figure 3. Local Bundle Adjustment is the most time-consuming stage in local mapping, accounting for approximately 60% to 75% of the total execution time, as shown in Figure 2. As discussed in Section II, several prior efforts have been made to accelerate this component due to its significant performance impact. Since this component has been extensively studied and optimized in prior work, we chose to adopt an existing implementation rather than develop a new one from scratch. Specifically, we integrate the GPU-accelerated local bundle adjustment from the work of Gopinath et al. [12], which is compatible with ORB-SLAM3. In this work, the *Schur Complement* method, which is used to reduce the system size and speed up the LBA process, is offloaded to the GPU. Their implementation serves as a drop-in replacement block solver for g2o [16], the optimization library used by ORB-SLAM3 for solving the local bundle adjustment problem.

F. Local Keyframe Culling

Local Keyframe Culling is the final major component of local mapping. TurboMap does not offload this stage to the GPU, mainly due to the significant data transfer overhead it would have. Instead, we apply a CPU-side optimization to improve its performance while avoiding the cost of GPU data transfers.

As described in Section III, the Keyframe Culling stage removes redundant keyframes by checking how many of their associated map points are also observed by other keyframes in the map at the same or finer scale, and discarding those that exceed a predefined threshold. To perform this check, the system maintains an observation list for each map point, which records the set of keyframes that observe that point. This data structure is large and frequently updated during each iteration of local mapping. Unlike the relatively static keyframe data which can be stored on the GPU without frequent synchronization, the dynamic nature of the observation data makes it unsuitable for the same treatment. We experimented with a GPU-side map point storage system that continuously updated this data, but found that maintaining consistency introduced significant overhead. In fact, the cost of keeping this storage synchronized was nearly equivalent to the total cost of the entire local mapping stage, making the approach impractical. As a result, we chose not to offload this component to the GPU.

Instead of offloading this logic to the GPU, we optimize it on the CPU by introducing a lightweight array that tracks how many times each map point is observed at each scale. Each time a map point is observed, the corresponding counter in the array is incremented. This approach eliminates the need to iterate over every keyframe’s observations to count the number of valid observations per map point. As a result, it significantly reduces the computational overhead of the keyframe culling process. The additional memory overhead of this optimization is minimal, as we store only a small

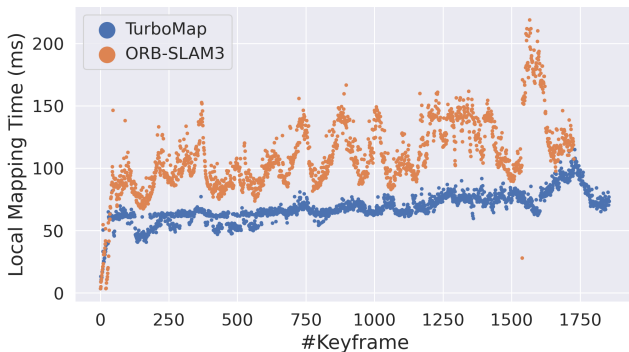


Fig. 4: Corridor1 keyframe processing time for TurboMap and ORB-SLAM3 in Desktop environment.

array per map point, which amounts to just a few bytes per map point.

V. EVALUATION

A. Experimental Setup

We evaluate the performance of TurboMap by running a set of sequences on two different hardware platforms and comparing the results with those of the original ORB-SLAM3. The experiments are conducted in two setups: a desktop machine and a mobile embedded system. The desktop system is equipped with a 20-core Intel Core i7-12700K CPU running at 5.0 GHz, an NVIDIA RTX 3090 GPU with 10,496 CUDA cores, and 64 GB of RAM. The embedded platform is a Jetson Xavier NX, featuring a 6-core ARM Carmel CPU running at 1.4 GHz (20W configuration), a 384-core NVIDIA Volta GPU, and 8 GB of RAM. To ensure consistent and reproducible results, we lock the CPU and GPU frequencies to their maximum values during all experiments.

For evaluation, we use a combination of sequences from the TUM-VI and EuRoC datasets, both in the stereo-inertial configuration. We run each sequence five times and report the average results across these runs to account for variability and ensure fair comparison.

B. Overall Performance

Table I presents the performance comparison between TurboMap and ORB-SLAM3 in different components of local mapping. As shown, TurboMap gets an average speedup of $1.3\times$ in EuRoC and $1.6\times$ in TUM-VI, in both the desktop and embedded settings. Importantly, TurboMap achieves these performance gains while maintaining a similar Absolute Trajectory Error (ATE) RMSE as ORB-SLAM3, demonstrating that our optimizations do not compromise the accuracy of the system.

In addition to improving the average processing speed, TurboMap also significantly reduces the standard deviation of keyframe processing times. This improvement indicates that keyframes are processed with more consistent latency,

reducing the occurrence of outlier frames that require significantly more time to process. As a result, fewer keyframes are at risk of being dropped due to excessive processing delays.

To illustrate the impact of reduced variance, Figure 4 shows the keyframe processing time for both systems in the corridor1 sequence. As the number of keyframes in the map increases, ORB-SLAM3 exhibits a noticeable growth in processing time per keyframe. This is due to the increased workload across components such as triangulation, fusion, and local bundle adjustment, all of which scale with map size. In contrast, TurboMap maintains stable processing times even as the map grows, thanks to its GPU-accelerated components and CPU-side optimizations that effectively distribute and manage the computational load. This effect is clearly visible when comparing the maximum keyframe processing times in both systems: approximately 220 ms for ORB-SLAM3 versus only 115 ms for TurboMap.

C. Individual Component Performances

We analyze the performance gains from each optimization introduced in TurboMap in the following subsections. It is important to note that the observed speedups differ between the EuRoC and TUM-VI datasets. This discrepancy arises from the different camera models and the way ORB-SLAM3 processes them. Specifically, in TUM-VI, which employs fisheye cameras, the system does not rectify the images. Instead, it treats the stereo pair as two independent monocular cameras in order to leverage the wider field of view and retain more detected features. As a result, TUM-VI sequences contain approximately twice as many map points as those in EuRoC. Consequently, local mapping components, particularly those that scale with the number of map points, require significantly more processing time in TUM-VI.

1) *Search for Triangulation*: The GPU optimization of the Search for Triangulation component results in an average speedup of $2.2\times$ on the EuRoC dataset and $3.3\times$ on the TUM-VI dataset in the desktop setting. In the Jetson setting, it achieves an average speedup of $3.5\times$ on EuRoC and $5.2\times$ on TUM-VI. The higher speedup achieved in TUM-VI is because the system is searching for more map point matches to triangulate in this dataset as we explained earlier, and TurboMap uses more GPU threads in this optimization compared to EuRoC, resulting in greater performance gains.

2) *Map Point Fusion*: Offloading the Map Point Fusion component to the GPU yields an average speedup of $1.5\times$ on the EuRoC dataset and $2.3\times$ on the TUM-VI dataset in the desktop setting. On the Jetson platform, it achieves average speedups of $1.4\times$ and $2.2\times$ on EuRoC and TUM-VI, respectively. The improved performance on TUM-VI is attributed to the higher number of map points being fused, allowing TurboMap to exploit parallelism more effectively by utilizing a greater number of GPU threads.

3) *Keyframe Culling*: TurboMap optimizes the Keyframe Culling process on the CPU, achieving an average speedup of $1.8\times$ on the EuRoC dataset in both desktop and Jetson

| Sequence | Total Local Mapping | | Speed Up | Triangulation | | Speed Up | Fusion | | Speed Up | LBA | | Speed Up | KF Culling | | Speed Up | ATE | |
|-------------------|---------------------|-----------|-------------|---------------|------|-------------|--------|-------|-------------|--------|--------|-------------|------------|-------|-------------|-------|-------|
| | Original | TurboMap | | Org | TM | | Org | TM | | Org | TM | | Org | TM | | Org | TM |
| EuRoC Avg | 372.70 | 287.90 | 1.3x | 7.10 | 2.04 | 3.5x | 38.06 | 27.72 | 1.4x | 276.37 | 218.28 | 1.3x | 31.60 | 17.45 | 1.8x | 0.034 | 0.031 |
| MH01 | 364 ± 139 | 278 ± 104 | 1.3x | 8.6 | 2.1 | 4.1x | 37.6 | 25.9 | 1.5x | 267.4 | 209.6 | 1.3x | 29.7 | 17.4 | 1.7x | 0.040 | 0.039 |
| MH02 | 322 ± 127 | 249 ± 95 | 1.3x | 8.0 | 2.2 | 3.7x | 33.2 | 22.7 | 1.5x | 238.7 | 188.8 | 1.3x | 23.9 | 14.1 | 1.7x | 0.032 | 0.032 |
| V101 | 425 ± 101 | 321 ± 75 | 1.3x | 5.7 | 1.9 | 3.0x | 43.1 | 31.7 | 1.4x | 313.8 | 243.9 | 1.3x | 42.0 | 20.6 | 2.0x | 0.038 | 0.038 |
| V102 | 379 ± 116 | 302 ± 95 | 1.3x | 6.1 | 2.0 | 3.1x | 38.4 | 30.5 | 1.3x | 285.6 | 230.8 | 1.2x | 30.7 | 17.7 | 1.7x | 0.027 | 0.018 |
| TUM-VI Avg | 551.63 | 356.85 | 1.6x | 33.68 | 6.45 | 5.2x | 90.42 | 40.79 | 2.2x | 342.99 | 257.45 | 1.3x | 55.49 | 17.43 | 3.2x | 0.013 | 0.013 |
| room1 | 584 ± 164 | 387 ± 103 | 1.5x | 30.3 | 5.8 | 5.3x | 106.1 | 48.2 | 2.2x | 356.8 | 278.6 | 1.3x | 59.0 | 16.3 | 3.6x | 0.008 | 0.009 |
| room2 | 529 ± 159 | 364 ± 118 | 1.5x | 29.8 | 5.6 | 5.4x | 89.3 | 42.2 | 2.1x | 337.0 | 265.4 | 1.3x | 43.6 | 14.2 | 3.1x | 0.011 | 0.012 |
| corridor1 | 546 ± 126 | 339 ± 63 | 1.6x | 36.5 | 7.2 | 5.1x | 82.6 | 36.4 | 2.3x | 339.8 | 244.2 | 1.4x | 60.9 | 19.8 | 3.1x | 0.015 | 0.017 |
| corridor2 | 545 ± 112 | 335 ± 57 | 1.6x | 38.1 | 7.3 | 5.2x | 83.7 | 36.4 | 2.3x | 338.3 | 241.6 | 1.4x | 58.4 | 19.5 | 3.0x | 0.020 | 0.018 |

(a) Jetson Results

| Sequence | Total Local Mapping | | Speed Up | Triangulation | | Speed Up | Fusion | | Speed Up | LBA | | Speed Up | KF Culling | | Speed Up | ATE | |
|-------------------|---------------------|-------------|-------------|---------------|------|-------------|--------|------|-------------|-------|-------|-------------|------------|------|-------------|-------|-------|
| | Original | TurboMap | | Org | TM | | Org | TM | | Org | TM | | Org | TM | | Org | TM |
| EuRoC Avg | 65.73 | 51.56 | 1.3x | 1.60 | 0.73 | 2.2x | 6.83 | 4.60 | 1.5x | 48.52 | 39.05 | 1.2x | 4.45 | 2.42 | 1.8x | 0.036 | 0.034 |
| MH01 | 65.0 ± 26.4 | 49.2 ± 18.7 | 1.3x | 1.8 | 0.7 | 2.6x | 6.7 | 4.3 | 1.6x | 47.0 | 36.8 | 1.3x | 4.9 | 2.6 | 1.9x | 0.042 | 0.036 |
| MH02 | 58.7 ± 24.1 | 45.1 ± 17.3 | 1.3x | 1.8 | 0.7 | 2.5x | 6.1 | 3.8 | 1.6x | 42.7 | 33.9 | 1.3x | 3.9 | 2.1 | 1.8x | 0.032 | 0.031 |
| MH03 | 70.1 ± 25.3 | 54.1 ± 19.4 | 1.3x | 1.7 | 0.7 | 2.4x | 7.4 | 4.7 | 1.6x | 51.9 | 41.3 | 1.3x | 4.6 | 2.6 | 1.8x | 0.034 | 0.030 |
| MH04 | 63.3 ± 20.1 | 51.8 ± 15.2 | 1.2x | 1.8 | 1.0 | 1.9x | 6.3 | 4.6 | 1.4x | 47.3 | 38.7 | 1.2x | 3.4 | 2.3 | 1.5x | 0.045 | 0.040 |
| MH05 | 63.8 ± 19.5 | 51.4 ± 14.9 | 1.2x | 1.8 | 1.0 | 1.8x | 6.4 | 4.5 | 1.4x | 47.6 | 38.4 | 1.2x | 3.4 | 2.2 | 1.5x | 0.054 | 0.054 |
| V101 | 77.2 ± 18.8 | 58.4 ± 14.1 | 1.3x | 1.3 | 0.5 | 2.4x | 8.0 | 5.4 | 1.5x | 56.6 | 44.6 | 1.3x | 6.7 | 3.0 | 2.3x | 0.038 | 0.038 |
| V102 | 69.7 ± 22.6 | 55.5 ± 17.7 | 1.3x | 1.4 | 0.6 | 2.4x | 7.2 | 5.1 | 1.4x | 52.2 | 42.8 | 1.2x | 4.9 | 2.6 | 1.9x | 0.018 | 0.018 |
| V103 | 58.0 ± 15.5 | 46.9 ± 11.7 | 1.2x | 1.2 | 0.6 | 2.1x | 6.5 | 4.5 | 1.5x | 43.0 | 35.9 | 1.2x | 3.9 | 2.1 | 1.8x | 0.026 | 0.026 |
| TUM-VI Avg | 109.81 | 69.84 | 1.6x | 7.68 | 2.36 | 3.3x | 17.88 | 7.63 | 2.3x | 67.06 | 49.10 | 1.4x | 10.43 | 3.16 | 3.3x | 0.012 | 0.013 |
| room1 | 113.2 ± 33.8 | 75.1 ± 19.6 | 1.5x | 7.1 | 2.1 | 3.3x | 19.8 | 9.0 | 2.2x | 68.9 | 52.8 | 1.3x | 10.3 | 3.0 | 3.5x | 0.009 | 0.013 |
| room2 | 103.2 ± 32.3 | 72.6 ± 20.3 | 1.4x | 7.2 | 2.0 | 3.5x | 16.9 | 7.8 | 2.1x | 64.6 | 52.1 | 1.2x | 7.9 | 2.7 | 3.0x | 0.012 | 0.012 |
| room3 | 111.5 ± 29.4 | 69.4 ± 14.6 | 1.6x | 7.3 | 2.1 | 3.5x | 16.9 | 6.9 | 2.5x | 73.1 | 50.7 | 1.4x | 7.8 | 2.5 | 3.2x | 0.009 | 0.014 |
| room4 | 101.9 ± 32.4 | 64.1 ± 14.3 | 1.6x | 7.0 | 2.2 | 3.2x | 18.1 | 7.3 | 2.5x | 60.7 | 44.7 | 1.4x | 9.1 | 2.4 | 3.7x | 0.009 | 0.009 |
| room5 | 112.6 ± 31.1 | 74.4 ± 17.4 | 1.5x | 7.3 | 2.3 | 3.3x | 19.7 | 8.8 | 2.3x | 68.1 | 52.3 | 1.3x | 10.3 | 3.0 | 3.5x | 0.011 | 0.012 |
| room6 | 114.7 ± 31.0 | 71.5 ± 16.6 | 1.6x | 6.8 | 2.1 | 3.2x | 21.6 | 9.8 | 2.2x | 67.5 | 48.0 | 1.4x | 10.9 | 2.7 | 4.0x | 0.006 | 0.006 |
| corridor1 | 110.6 ± 28.8 | 67.8 ± 12.3 | 1.6x | 8.6 | 2.8 | 3.1x | 15.8 | 6.3 | 2.5x | 67.4 | 47.7 | 1.4x | 12.5 | 4.1 | 3.0x | 0.020 | 0.021 |
| corridor2 | 110.3 ± 25.5 | 66.5 ± 10.4 | 1.7x | 8.9 | 2.9 | 3.1x | 15.9 | 6.2 | 2.6x | 67.2 | 46.7 | 1.4x | 12.2 | 4.0 | 3.1x | 0.019 | 0.016 |
| corridor3 | 110.3 ± 28.3 | 67.0 ± 11.5 | 1.6x | 8.9 | 2.8 | 3.2x | 16.1 | 6.5 | 2.5x | 66.1 | 46.8 | 1.4x | 12.9 | 4.2 | 3.1x | 0.009 | 0.014 |

(b) Desktop Results

TABLE I: Performance comparison of TurboMap and ORB-SLAM3 using the desktop and Jetson setups on EuRoC and TUM-VI datasets. We report mean±std runtime (ms), speed-up, and ATE RMSE (m).

settings. In the TUM-VI dataset, it achieves a speedup of 3.3× in the desktop setting and 3.2× in Jetson.

D. Trajectory

Table I compares the Absolute Trajectory Error (ATE) RMSE between TurboMap and ORB-SLAM3. As shown, both systems achieve comparable accuracy across all sequences, demonstrating the robustness of TurboMap in correctly processing keyframes. Figure 5 visualizes the esti-

ated trajectories for both systems in the corridor1 sequence. The trajectories closely align, indicating that TurboMap preserves the localization accuracy of ORB-SLAM3.

E. Stress Testing Local Mapping

To investigate system performance under rapidly changing scenes, we design an experiment that simulates scenarios requiring a high keyframe insertion rate to maintain tracking accuracy. This experiment enables us to evaluate how

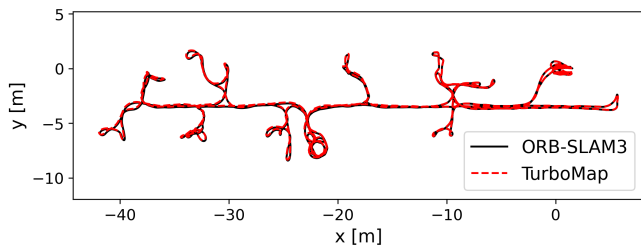


Fig. 5: Trajectory comparison between TurboMap and ORB-SLAM3 in corridor1.

| Sequence | TurboMap | | ORB-SLAM3 | |
|-----------|----------|---------------------------|-----------|---------------------------|
| | ATE | #Skipped LBA & KF Culling | ATE | #Skipped LBA & KF Culling |
| MH01 | 0.040 | 3.4 | 1.105 | 58 |
| V101 | 0.039 | 18.8 | 0.091 | 102.6 |
| room1 | 0.011 | 5.8 | 1.005 | 140.4 |
| corridor1 | 0.045 | 9.2 | 10.136 | 343.8 |

TABLE II: Comparison of TurboMap and ORB-SLAM3 under high keyframe insertion, showing ATE RMSE (m) and the number of skipped Local Bundle Adjustments/Keyframe Cullings across sequences in the desktop setting, averaged over 5 runs.

TurboMap and ORB-SLAM3 perform under a heavy local mapping load. To do that, we simulate a sequence with high camera motion. Rapid camera motion can cause substantial changes in the observed scene between consecutive frames due to large viewpoint shifts and motion blur, resulting in previously tracked features becoming unobservable or unrecognizable. If keyframes are inserted too sparsely, the viewpoint difference between keyframes becomes large, making descriptor matching and triangulation less reliable. More frequent keyframe insertion shortens this difference, preserves sufficient feature overlap for robust matching, and helps maintain tracking accuracy under fast motion. Typically, more frequent keyframe insertion improves tracking robustness under challenging camera motion [2].

To achieve higher keyframe insertion rates, we apply two modifications to both systems. First, ORB-SLAM3 includes a limiter that enforces real-time playback by pausing execution when tracking processes a frame faster than the sequence timestamp. We disable this limiter to accelerate frame processing and thereby simulate high camera velocity. Second, ORB-SLAM3 enforces a minimum frame interval between consecutive keyframe insertions. We reduce this threshold to permit denser keyframe insertion when rapid motion requires it. Together, these modifications increase the load on local mapping and enable a direct evaluation of the robustness and scalability of TurboMap relative to ORB-SLAM3.

As shown in Table II, TurboMap significantly outperforms ORB-SLAM3 under heavy load. While ORB-SLAM3 pro-

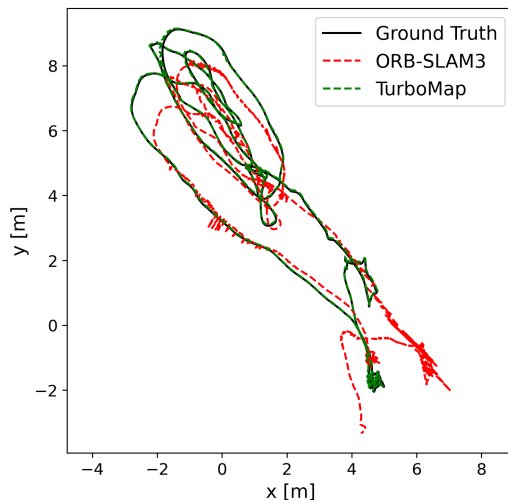


Fig. 6: Trajectory comparison in MH01 between TurboMap and ORB-SLAM3 under a high keyframe insertion rate.

duces very high absolute trajectory errors (ATE), TurboMap maintains an accuracy comparable to normal load conditions, which is substantially lower than the error in ORB-SLAM3. This difference is also evident in Figure 6, where the trajectory produced by ORB-SLAM3 in the MH01 sequence diverges significantly from the ground truth, while TurboMap produces a trajectory that closely aligns with it. This discrepancy can be explained by the way ORB-SLAM3 manages new keyframes. The local mapping module maintains a fixed-size keyframe queue and processes keyframes sequentially. When the queue is not empty, ORB-SLAM3 skips Local Bundle Adjustment and Keyframe Culling stages for the current keyframe and starts processing the next keyframe in the queue in order to save time and avoid keyframe drops. However, skipping these stages directly impacts trajectory accuracy. Table II further illustrates this point by reporting the number of times LBA and Keyframe Culling are skipped under heavy load in both systems. The number of skips is substantially higher in ORB-SLAM3, which is the primary factor contributing to its decreased accuracy.

VI. CONCLUSION

In this work, we present TurboMap, a GPU-accelerated and CPU-optimized backend for ORB-SLAM3 designed to address key performance bottlenecks in the local mapping process. TurboMap leverages GPU parallelism to accelerate the Search for Triangulation and Map Point Fusion stages, introduces an efficient CPU-side optimization for Keyframe Culling, incorporates an existing GPU-accelerated implementation of Local Bundle Adjustment, and minimizes data transfer overhead by employing GPU-resident keyframe storage. Collectively, these enhancements yield an average speedup of $1.3\times$ in the EuRoC dataset and $1.6\times$ in the TUM-VI dataset in local mapping. One limitation of the proposed approach is the overhead associated with transferring data to GPU memory, which can introduce latency. However, on platforms such as NVIDIA Jetson, where the CPU and GPU

share a unified memory architecture, this overhead is largely eliminated. This highlights the potential for even greater performance gains on embedded platforms where memory sharing allows for more efficient parallel computation without the cost of data migration.

REFERENCES

- [1] S. Semenova, S. Ko, Y. D. Liu, L. Ziarek, and K. Dantu, "A comprehensive study of systems challenges in visual simultaneous localization and mapping systems," *ACM Trans. Embed. Comput. Syst.*, vol. 24, no. 1, Sept. 2024. [Online]. Available: <https://doi.org/10.1145/3677317>
- [2] R. Mur-Artal, J. M. M. Montiel, and J. D. Tardos, "Orb-slam: A versatile and accurate monocular slam system," *IEEE Transactions on Robotics*, vol. 31, no. 5, p. 1147–1163, Oct. 2015.
- [3] R. Mur-Artal and J. D. Tardos, "Orb-slam2: An open-source slam system for monocular, stereo, and rgb-d cameras," *IEEE Transactions on Robotics*, vol. 33, no. 5, p. 1255–1262, Oct. 2017.
- [4] C. Campos, R. Elvira, J. J. G. Rodriguez, J. M. M. Montiel, and J. D. Tardos, "Orb-slam3: An accurate open-source library for visual, visual-inertial, and multimap slam," *IEEE Transactions on Robotics*, vol. 37, no. 6, p. 1874–1890, Dec. 2021.
- [5] P. Geneva, K. Eickenhoff, W. Lee, Y. Yang, and G. Huang, "Openvins: A research platform for visual-inertial estimation," in *2020 IEEE International Conference on Robotics and Automation (ICRA)*, 2020, pp. 4666–4672.
- [6] A. Rosinol, M. Abate, Y. Chang, and L. Carlone, "Kimera: an open-source library for real-time metric-semantic localization and mapping," in *2020 IEEE International Conference on Robotics and Automation (ICRA)*, 2020, pp. 1689–1696.
- [7] M. Burri, J. Nikolic, P. Gohl, T. Schneider, J. Rehder, S. Omari, M. W. Achtelik, and R. Siegwart, "The euroc micro aerial vehicle datasets," *The International Journal of Robotics Research*, 2016. [Online]. Available: <http://ijr.sagepub.com/content/early/2016/01/21/0278364915620033.abstract>
- [8] D. Schubert, T. Goll, N. Demmel, V. Usenko, J. Stückler, and D. Cremers, "The tum vi benchmark for evaluating visual-inertial odometry," in *2018 IEEE/RSJ International Conference on Intelligent Robots and Systems (IROS)*, 2018, pp. 1680–1687.
- [9] S. Aldegheri, N. Bombieri, D. D. Bloisi, and A. Farinelli, "Data flow orb-slam for real-time performance on embedded gpu boards," in *2019 IEEE/RSJ International Conference on Intelligent Robots and Systems (IROS)*. Macau, China: IEEE, Nov. 2019, p. 5370–5375. [Online]. Available: <https://ieeexplore.ieee.org/document/8967814/>
- [10] A. Kumar, J. Park, and L. Behera, "High-speed stereo visual slam for low-powered computing devices," *IEEE Robotics and Automation Letters*, vol. 9, no. 1, p. 499–506, Jan. 2024.
- [11] K. Khabiri, P. Hosseinijad, S. Gopinath, K. Dantu, and S. Y. Ko, "Fasttrack: Gpu-accelerated tracking for visual slam," 2025. [Online]. Available: <https://arxiv.org/abs/2509.10757>
- [12] S. Gopinath, K. Dantu, and S. Y. Ko, "Improving the performance of local bundle adjustment for visual-inertial slam with efficient use of gpu resources," in *2023 IEEE International Conference on Robotics and Automation (ICRA)*, 2023, pp. 6239–6245.
- [13] D. Kumar, S. Gopinath, K. Dantu, and S. Y. Ko, "Jacobigpu: Gpu-accelerated numerical differentiation for loop closure in visual slam," in *2024 IEEE International Conference on Robotics and Automation (ICRA)*, 2024, pp. 1687–1693.
- [14] S. Agarwal, K. Mierle, and T. C. S. Team, "Ceres Solver," 10 2023. [Online]. Available: <https://github.com/ceres-solver/ceres-solver>
- [15] J. Ren, W. Liang, R. Yan, L. Mai, S. Liu, and X. Liu, "Megba: A gpu-based distributed library for large-scale bundle adjustment," 2022. [Online]. Available: <https://arxiv.org/abs/2112.01349>
- [16] R. Kümmerle, G. Grisetti, H. Strasdat, K. Konolige, and W. Burgard, "G2o: A general framework for graph optimization," in *2011 IEEE International Conference on Robotics and Automation*, 2011, pp. 3607–3613.